APPLIED ORGANOMETALLIC CHEMISTRY, VOL. 11, 181–194 (1997)

Synthesis and Characterization of Silazane-Based Polymers as Precursors for Ceramic Matrix Composites

J. Lücke, J. Hacker, D. Suttor and G. Ziegler†
Institute of Materials Research, Department of Ceramics and Composites, University of Bayreuth, D-95440 Bayreuth, Germany

The goal of this investigation was to optimize the synthesis of silazane-based polymers for processing fibre-reinforced ceramic matrix composites (CMCs). Liquid oligomeric silazanes were synthesized by ammonolysis of chlorosilanes and characterized spectroscopically (FTIR, NMR) as well as by elemental analysis. The silazanes were obtained in high yield and purity. Different functional groups (system S1: Si—H, Si—CH_3, Si—$CH=CH_2$) and different degrees of branching in the Si—N backbone [system S2; $Si(NH)_3$, $Si(NH)_2$] were realized in order to study the properties of the silazanes that are dependent on the molecular structure.

For processing ceramics via pyrolysis of pre-ceramic oligomers, molecular weight, rheological behaviour, thermosetting and ceramic yield were investigated systematically and correlated with the molecular structure of the silazanes. Low molecular weights (500–1000 g mol^{-1}) as well as low viscosity values (0.1–20 Pa s) enable processing of the silazanes in the liquid phase without any solvent. Due to the latent reactivity of the functional groups, curing of the polymers via hydrosilylation is achieved.

Structural changes and weight loss during polymer curing as well as the organic/inorganic transition were monitored by FTIR spectroscopy and differential thermogravimetric analysis. With increasing temperature (room temperature to 800 °C) the hydrogen content decreases from 7 to < 0.5 wt% due to the formation of gaseous molecules (NH_3, CH_4, H_2). High ceramic yields up to 80% were reached by branching the oligomers, thus reducing the amount of volatile precursor fragments.

Up to 1300 °C, ceramic materials remained amorphous to X-rays. At higher temperatures (1400–1800 °C) either SiC or SiC/Si_3N_4 composites were selectively crystallized, depending on the pyrolysis conditions. The utility of the optimized precursors for CMCs has been demonstrated by infiltration of fibre preforms and subsequent pyrolysis. © 1997 by John Wiley & Sons, Ltd.

Keywords: synthesis; silazanes; polymer pyrolysis; non-oxide ceramics; Si_3N_4; SiC; crystallization; ceramic matrix composites

INTRODUCTION

With the need for the development of non-oxide-based advanced ceramics, organometallic compounds have been investigated during recent years for their use as starting compounds for ceramics via the pyrolysis of these materials.[1] Today, pre-ceramic compounds (precursors) exist for various ceramic matrices, e.g. carbides and nitrides of boron, aluminium, silicon, titanium and other metals.[2,3]

For the preparation of SiC/Si_3N_4 ceramics, silazane-based precursors are necessary. Compounds with bonds between silicon and nitrogen were first investigated by Stock and co-workers.[4] In the 1960s, the main interest was focused on the chemical properties.[5,6] Polymer and ceramic aspects such as polymerization and curing, as well as pyrolysis and crystallization behaviour, have been analysed since 1973—but more qualitatively—when the usefulness of silazanes for producing ceramic fibres was demonstrated.[7] The first commercially available product was a silicon carbide fibre made from polycarbosilanes (Nicalon™, Nippon Carbon), a result of the research work of Yajima and co-workers.[8] Several researchers summarized the results on

† Author to whom correspondence should be addressed.

CCC 0268–2605/97/020181–14

Received 12 March 1996
Accepted 4 June 1996

silazanes.[9–11] They stated that a useful organometallic pre-ceramic compound should be liquid, fusible and/or soluble to be processable. A general property required is a high ceramic yield which necessitates crosslinking of the synthesized liquid oligomers.[12a] The corresponding crosslinked polymers are usually solid or even insoluble and thus untractable. To make use of the shaping capabilities with respect to polymer processing, this step requires setting of the oligomers after forming. This requires latent reactivity for curing to an unmeltable resin. Additionally, a certain degree of crosslinking even in the molecular oligomers is necessary to prevent chain scission and back-biting with the subsequent evolution of low-molecular volatile fragments.[13] This is usually the case when linear polymers are pyrolysed. Furthermore, pyrolysis should result in a ceramic material with the desired chemical composition and microstructure. To control the various demands with respect to processing of ceramic composites, e.g. high ceramic yield, low viscosity and shaping capabilities, and to realize them preferably in one molecule, is still an ambitious aim.

Depending on their physical state (solid, liquid), different processing techniques have been developed to make organometallic compounds useful for shaping ceramic materials and components. Very few attempts have been successful in making dense and crackfree monolithic or composite materials.[14, 15] Fibre spinning, coating, usage as a binder and infiltration of porous materials (porous ceramics, fibre preforms) have been applied,[2] focusing on silicon carbide/nitride materials. Building up the matrix of ceramic matrix composites by infiltration of porous fibre preforms opens a very promising way to produce fibre-reinforced ceramics without fibre damage,[16] and thus to overcome the brittle fracture usually observed in monolithic ceramics. The fabrication of CMCs includes the liquid impregnation of fibre preforms with suitable precursors (e.g. low-viscosity, solvent-free) followed by subsequent crosslinking to thermosets and pyrolysis at temperatures above 300 °C. Compared with the usual processing techniques for ceramic materials, this procedure is a low-temperature, pressureless process making it possible to manufacture complex shaped parts without damage to the fibres, either chemical or mechanical.[17]

The aim of this work was to optimize the molecular structure of the precursors for preparation of Si_3N_4/SiC ceramics and to control the organic/inorganic transition. In this context, particularly with respect to the development of CMCs, oligomeric silazanes were developed with different chemical compositions containing unbranched (system S1) or branched (system S2) cyclic silazanes with $[SiR_2—NH—]_n$ units.

EXPERIMENTAL PROCEDURE

Most of the starting materials as well as the synthesized silazanes are sensitive to moisture and air. Thus, all operations, e.g. synthesis, purification, characterization as well as further processing, were carried out in an inert gas atmosphere (vacuum line, Schlenk technique, glovebox) to avoid oxygen impurities. Nitrogen and argon (>99.998%) were purified by passing through successive columns of potassium hydroxide, siccapent™, and BTS catalysts. Flasks were evacuated (<1 Pa) and filled with dried argon before use. The solvents (toluene and *p*-xylene, p.a., Merck) were refluxed and distilled from molten sodium. The chlorosilanes (97–99%) were distilled; ammonia was used in the as-received state (>99.995%). Chemical analysis (Si, N, C, H, Cl, O) was carried out by Pascher Microanalytical Laboratory (Remagen, Germany).

The silazanes (pure liquids) as well as the resulting pyrolysed materials were investigated by FTIR spectroscopy. Liquid samples (FTS 15/80, Biorad) were analysed between KBr plates, solids (IFS 66v, Bruker) as pellets diluted (1:500) in 0.5 g potassium bromide. Transition mode was used in the wavenumber range 4000–400 cm^{-1} (resolution 1 cm^{-1}; measuring time 300 s). NMR spectra of the liquid silazanes were recorded in solution (≈10 vol% in C_6D_6) using a Bruker ARX 250 spectrometer (frequency: ^1H 250 MHz; ^{29}Si 50 MHz). Residual C_6H_6 was used as the internal reference.

Rheological measurements were performed on a cone–plate viscometer Rheolab MC 10 (Physica Meßtechnik) with about 2 g of sample material. At a controlled temperature, viscosity values were determined by measuring the shear stress as a function of shear rate. The influence of temperature and time on the viscosity was investigated. The viscometer was calibrated with silicone oils (100 BW and 20000 AW, Orwo Calibration Service).

Molecular weights were determined cryoscopically. The samples (1–3 g) were dissolved in 75 ml of *p*-xylene (p.A.; melting point of pure solvent 13.26 °C, $K_{cryos} = 4.3$ K kg mol^{-1}) and the freezing-point depression was measured for three concentrations (molality 0.02–0.12). Three commercially available silazanes [1, 1, 3, 3, 5, 5-hexamethylcyclotrisilazane and 1,3,5-trimethyl-1,3,5-trivinylcyclotrisilazane (ABCR), NCP200 (Nichimen)] were used for verification of the cryoscopic constant.

Thermal investigations (sample weight 25 mg; alumina crucible) were performed from room temperature up to 1000 °C in a thermal balance (STA409, Netzsch) coupled with a mass spectrometer. The heating rate was 5 K min^{-1} (argon atmosphere; flow rate 150 ml min^{-1}). Further weight loss of the pyrolysed samples was detected by weighing the samples before and after heating in a graphite chamber furnace (1000–1800 °C; heating rate 10 K min^{-1}; flow rate 150 ml min^{-1}).

The residues obtained after pyrolysis were ground to a fine powder and pressed into a cylindrical specimen holder (dia. 25 mm). X-ray powder diffraction patterns were recorded using $CuK_{\alpha 1}$ radiation ($\lambda = 154.06$ pm) on a Seifert XRD3000P powder diffractometer in Bragg–Brentano mode with a quartz single-crystal monochromator. Intensities were measured with a scintillation counter (step width: $2\theta = 0.02°$).

RESULTS AND DISCUSSION

Two systems were investigated to compare the properties of the silazanes. First, various functional groups were introduced (silazanes **S1a**–**S1d**); see Table 1) in the silzane backbone to control the reactivity (long-term stability, curing). In the second system (silazanes **S2a**–**S2e**; see Table 1) the molecular structure was changed by branching (10–70%) to modify molecular weight and viscosity.

Synthesis of silazanes

All silazanes were prepared by ammonolysis of chlorosilanes. Different functional groups attached to the Si—N backbone were introduced by varying the starting chlorosilanes. To achieve various ratios, mixtures of different silanes were employed. Equation [1] represents the overall reaction schematically.

$$R_z SiCl_{4-z} + 1.5(4-z)NH_3 \rightarrow 1/n\,[-R_z Si(NH)_{(4-z)/2}]_n + (4-z)NH_4Cl \quad [1]$$

$$R = H,\ CH_3,\ CH{=}CH_2$$

Monochlorosilane ($z = 3$): chain stopper
Dichlorosilane ($z = 2$): chains and rings
Trichlorosilane ($z = 1$): branching of silazanes

Formally, every chlorine atom is substituted by an NH_2 group followed by condensation to yield Si–NH–Si units. Ammonium chloride is formed from hydrogen chloride and excess ammonia. The parameter z may be varied by mixing different chlorosilanes. For $z = 2$ rings and chains are formed, whereas with decreasing z more and more branching of the molecules is expected. For $z = 0$ (no functional groups) the ammonolysis results in an untractable solid which is well known from the production of silicon nitride powder (diimide process).

For each reaction, 0.5 mol chlorosilane was dissolved in 600 ml toluene. Under vigorous mechanical stirring gaseous ammonia was passed through a glass capillary. Within half an hour, the temperature rose to 60 °C. The flow rate was then controlled in such a way that the temperature of the reaction mixture was held constant at 60 °C. After about 3 h, the exothermic reaction came to an end. The oil-bath temperature was held at 60 °C and excess ammonia was eliminated by passing argon through the suspension obtained. After the suspension had been filtered, the solvent was removed under reduced pressure (< 5 Pa). The resulting silazanes were colourless and liquid. The variation of functional groups and the yields of silazanes are summarized in Table 1.

The yield of liquid and soluble compounds amounted to 70–80 wt% relative to the theoretical value calculated from Eqn [1]. In general, the synthesis yield was reduced (5–10 wt%) by volatile compounds, mainly small rings, which were evaporated on removing the solvent. Furthermore, soluble precursor molecules which remained in the precipitated NH_4Cl could be obtained by extracting the residue more than twice. Insoluble products could be separated from the ammonium chloride only with considerable effort. The silazanes were sensitive to air and moisture and were kept in an argon atmosphere to avoid undesirable reactions (aging, oxygen impurities).

The chemical composition of the unbranched

Table 1 Functional groups and yields of the synthesized silazanes

	$[—SiR^1R^2—NH]_x/[—NHR^3]_y$				Ratio	Yield
	R^1	R^2	R^3	x/y	Si/N	(wt%)
S1a	CH_3	CH_3	—	—	1:1	50
S1b	H	CH_3	—	—	1:1	65
S1c	$CH=CH_2$	CH_3	—	—	1:1	91
S1d	$CH=CH_2$	CH_3	$SiHCH_3$	1:1	1:1	76
S2a	$CH=CH_2$	NH	$SiHCH_3$	1:10	1:1.05	73
S2b	$CH=CH_2$	NH	$SiHCH_3$	1:5	1:1.08	77
S2c	$CH=CH_2$	NH	$SiHCH_3$	1:2	1:1.17	75
S2d	$CH=CH_2$	NH	$SiHCH_3$	1:1	1:1.25	78
S2e	$CH=CH_2$	NH	$SiHCH_3$	1:0.5	1:1.33	74

silazanes was in the expected ratio (see also NMR results) whereas chemical analysis of the branched molecules showed a slightly higher C/N ratio than was calculated from the amounts of the educts with the assumption of a complete substitution of each chlorine atom by $(NH)_{1/2}$ (Table 2; see also Eqn [1]).

Oxygen and chlorine impurities could not be detected (detection limits: <0.5 wt% oxygen, <0.1 wt% chlorine). The lower nitrogen content may be explained by transamination reactions ($3\ NHSi_2 \rightarrow 2\ NSi_3 + NH_3$) occurring during synthesis and/or evaporation of the solvent.

NMR and FTIR spectroscopy

The solution ^1H spectrum of the precursor **S1d**, shown in Fig. 1, is typical for a cyclic unbranched silazane. ^1H signals were detected at 0.05–0.15 ppm ($\equiv Si—C\underline{H}_3$), 0.2–0.9 ppm (Si—N<u>H</u>—Si), 4.45–5.1 ppm (Si—<u>H</u>), 5.55–5.95 ppm ($\equiv Si—CH=C\mathbf{H}_2$), and 6.00–6.25 ppm ($\equiv Si—C\mathbf{H}=CH_2$). The deconvolution of the pattern was difficult, particularly for mixtures of silazanes. After ammonolysis of the chlorosilanes, condensation processes took place which led to a mixture of cyclic silazanes with diffeent ring sizes, in contrast to the formation of linear polymers from dichlorosilanes by reductive coupling with sodium. These cyclic compounds may have both different numbers of constituent elements (3,4,5, . . . $[SiR_2—NH–]$ units) and different substitution patterns.

Two multiplets appeared in the ^{29}Si NMR spectrum at about -15 ($H\underline{Si}CH_3$) and —22 ppm ($CH_3\underline{Si}CH=CH_2$] indicating mainly cyclic molecules, but the broad signals could not be resolved well and deconvolution into the individual isomers was not possible. In the case of branched silazanes, broad signals were detected even in the ^1H NMR spectra (Fig. 2) due to the higher number of possible isomers.

The intensities of the ^1H signals were in the appropriate ratio calculated from Eqn [1]. Thus, the substituents on the silicon atoms remained unreacted. Only small amounts of the solvent

Table 2 Chemical analysis of branched silazanes

	Analysis: Found (calcd.) (wt%)			
	S2a	**S2b**	**S2d**	**S2e**
Si	47.6 (46.2)	45.9 (45.1)	41.1 (41.1)	39.3 (39.3)
C	23.3 (21.5)	25.1 (22.5)	28.5 (26.3)	29.5 (28.0)
N	19.2 (24.1)	19.6 (24.4)	23.8 (25.6)	24.9 (26.1
H	8.0 (8.2)	7.8 (8.0)	6.8 (7.0)	6.5 (6.6)
O	<0.5 (0.0)	<0.5 (0.0)	<0.5 (0.0)	<0.5 (0.0)
Cl	<0.1 (0.0)	<0.1 (0.0)	<0.1 (0.0)	<0.1 (0.0)
Empirical formula	$SiC_{1.19}N_{0.81}H_{4.68}$ ($SiC_{1.09}N_{1.05}H_{4.95}$)	$SiC_{1.28}N_{0.86}H_{4.72}$ ($SiC_{1.17}N_{1.08}H_{4.92}$)	$SiC_{1.62}N_{1.16}H_{4.64}$ ($SiC_{1.50}N_{1.25}H_{4.75}$)	$SiC_{1.76}N_{1.27}H_{4.60}$ ($SiC_{1.67}N_{1.33}H_{4.67}$)

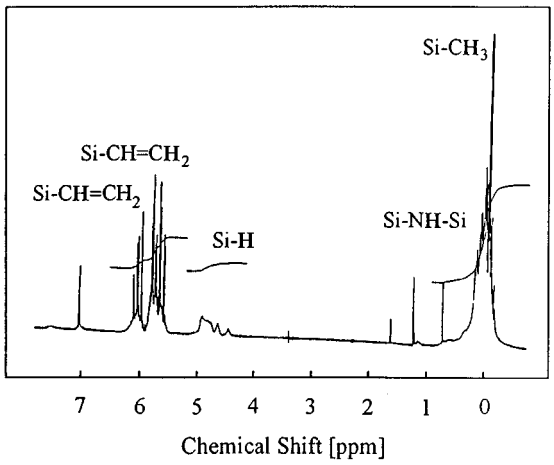

Figure 1 ^{1}H NMR spectrum of the unbranched silazane **S1d** ($SiH + SiCH=CH_2$).

were detectable (< 1%), even when highly viscous silazanes were synthesized.

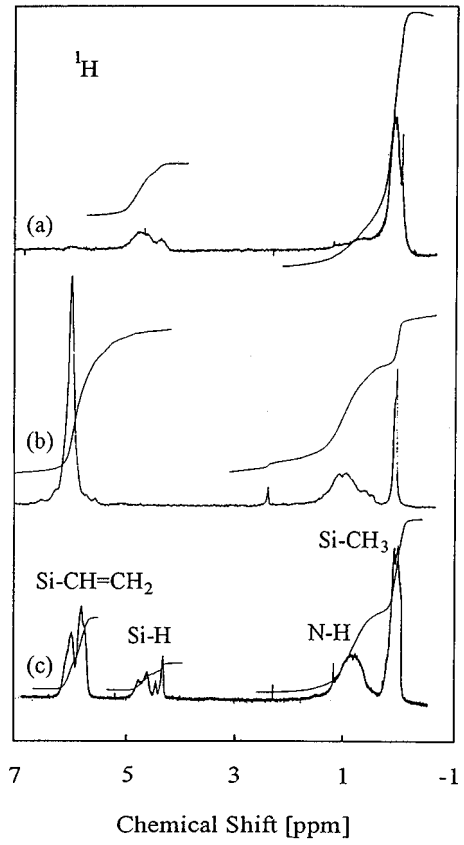

Figure 2 ^{1}H NMR spectra of branched silazanes with different functional groups: (a) Si—H; (b) $Si—CH=CH_2$; (c) $Si—H + Si—CH=CH_2$.

Functional groups were identified by infrared spectroscopy, too. Stretching vibrations of hydrogen bonds to nitrogen (3400–3385 cm^{-1}), to carbon [$3008 + 3049\ cm^{-1}$ (vinyl) and $2899 + 2960\ cm^{-1}$ (methyl)], and to silicon (2125) were detected (Fig. 3). Bands resulting from vinyl and methyl groups bonded to silicon appeared at $1600 + 1400\ cm^{-1}$ and $1255\ cm^{-1}$, respectively. The band at $1173\ cm^{-1}$ was assigned to an NH unit bridging two silicon atoms. In the wavenumber region below $1000\ cm^{-1}$, absorption bands of the stretching and deformation vibrations (Si—C, Si—N, C—H, C—C) were superimposed and could not be assigned unambiguously.

With increasing amounts of trifunctional silicon atoms (corresponding to the amount of trichlorosilane used for the synthesis), branching of the silazane rings appeared. The degree of

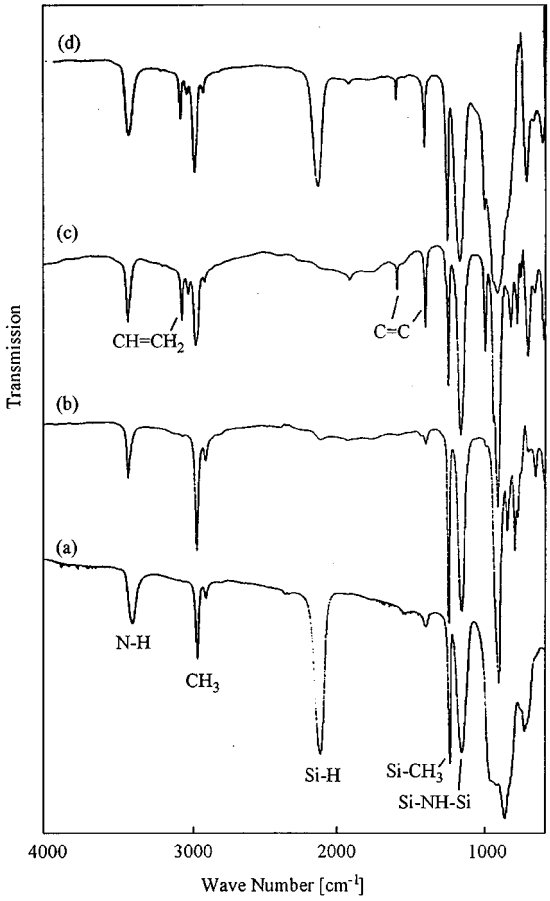

Figure 3 FTIR spectra of unbranched silazanes with different functional groups: (a) Si—H; (b) only CH_3; (c) $Si—CH=CH_2$; (d) $Si—H + Si—CH=CH_2$.

branching (D.B. = $RSi(NH)_{3/2}/R_2(NH)_{2/2}$) was calculated from the ratio of chlorosilanes used in the synthesis. As expected, the intensities of NH and $CH=CH_2$ absorption bands increased with a rise in the degree of branching (Fig. 4). Additionally, the Si—NH—Si absorption band split in two (1190 + 170 cm^{-1}).

Molecular weight and rheological behaviour

For processing pre-ceramic polymers in the liquid phase, special properties are required. To prove the utility of the synthesized silazanes, the more materials-relevant properties, (besides molecular weight), such as rheological behaviour and long-term stability, were determined. These properties are especially important for the development of ceramic matrix composites via infiltration of porous ceramics of fibre preforms.

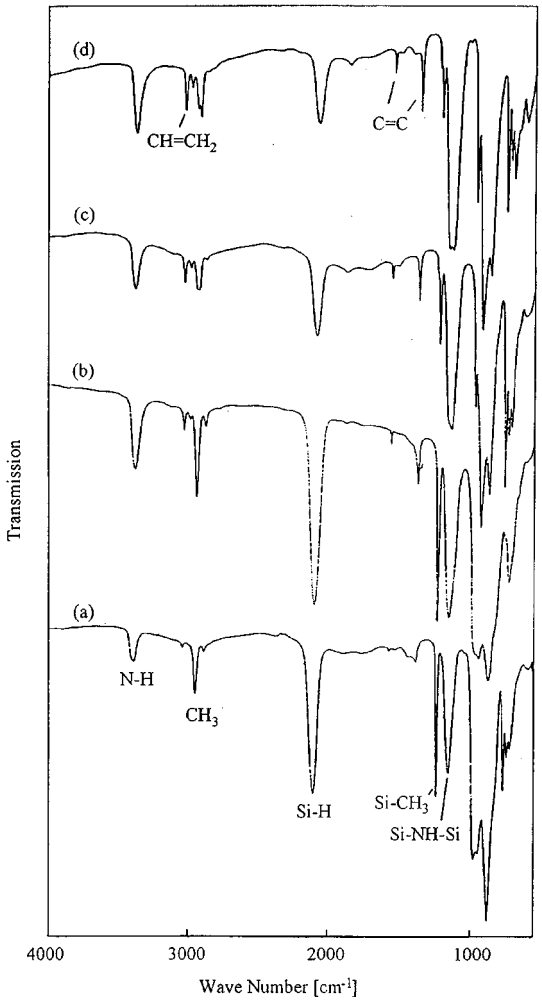

Figure 4 FTIR spectra of silazanes with different degrees of branching: (a) **S2a**, 1:10; (b) **S2b**, 1:5; (c) **S2d**, 1:1; (d) **S2e**, 1:0.5.

Table 3 Molecular weight (MW) and viscosity (η) of the unbranched (**S1a**–**S1d**) and branched silazanes (**S2a**–**S2e**)

	D.B.[a]	η (Pa s)	MW (g mol^{-1})	n[b]
S1a	—	(Solid)	238	3.2
S1b	—	0.012	383	6.5
S1c	—	0.004	234	2.7
S1d	—	0.007	333	4.6
S2a	1:10	0.25	498	8.2
S2b	1:5	0.84	529	8.5
S2c	1:2	1.42	560	8.6
S2d	1:1	17.0	619	9.0
S2e	1:0.5	23.7	806	11.3

[a] D.B., degree of branching, calculated from the ratio of educts (mean values).
[b] n, number of [SiR_2—NH—] units.

With the exception of precursor **S1a**, the synthesized silazanes were liquid at room temperature and miscible. The results of the cryoscopic measurements are shown in Table 3. With regard to the different weights of the substituents, the average number of monomeric [SiR_2—NH—] units was calculated from the molecular weight for better comparison. The molecular weight of the unbranched silazanes (precursors **S1a**–**S1d**) indicated the presence of small cyclic compounds composed of three to six monomeric units. The influence of the different substituents with respect to the molecular weight was small. However, for $R^1 = R^2 = CH_3$ (precursor **S1a**) the polymer was a solid at room temperature, probably due to the high proportion of tetrameric molecules (T_m = 97 °C). The influence of branching (precursors **S2a**–**S2e**; Table 3) was much more significant. Here, the molecular weight could be inceased from 5 up to 12 units, and may be controlled by the ratio of the starting chlorosilanes.

Viscosity values also were mainly dependent on the structure of the silazanes. With an increasing degree of branching, the viscosity increased from 0.01 to 25 Pa s (Table 3). Unbranched compounds exhibited low viscosity values with no significant changes if the substituents on the silicon atoms were varied. For a Newtonian fluid, the viscosity should be independent of the shear rate; this was the case for

silazanes with a D.B. of <50% (η=0.005–5.0 Pa s; see Fig. 5a). At higher degrees of branching (D.B. ⩾50%) the viscosity became more and more shear-rate-dependent (non-Newtonian fluid; Fig. 5b, c).

Viscosity values of ⩽20 Pa s at room temperature were sufficient for the infiltration of porous materials. If the flow behaviour was non-Newtonian, the temperature was raised to appropriate values. First of all, viscosity dropped exponentially with increasing temperature (Fig. 6a). After passing through a minimum at about 120 °C, the values increased rapidly. Above 200 °C the silazanes became solid. Even after an isothermal hold (2 h, 120 °C) the viscosity rose to much higher values than those suitable for infiltration techniques (Fig. 6b), resulting in solid materials. The unbranched silazanes were not sensitive (**S1a**+**S1c**), or even less sensitive (**S1d**, 150 °C, 24 h: 0.007→0.208 Pa s), to temperature with respect to viscosity.

Branched precursors exhibited long-term stability up to 60 °C; at higher temperatures crosslinking of the silazanes took place. Apart

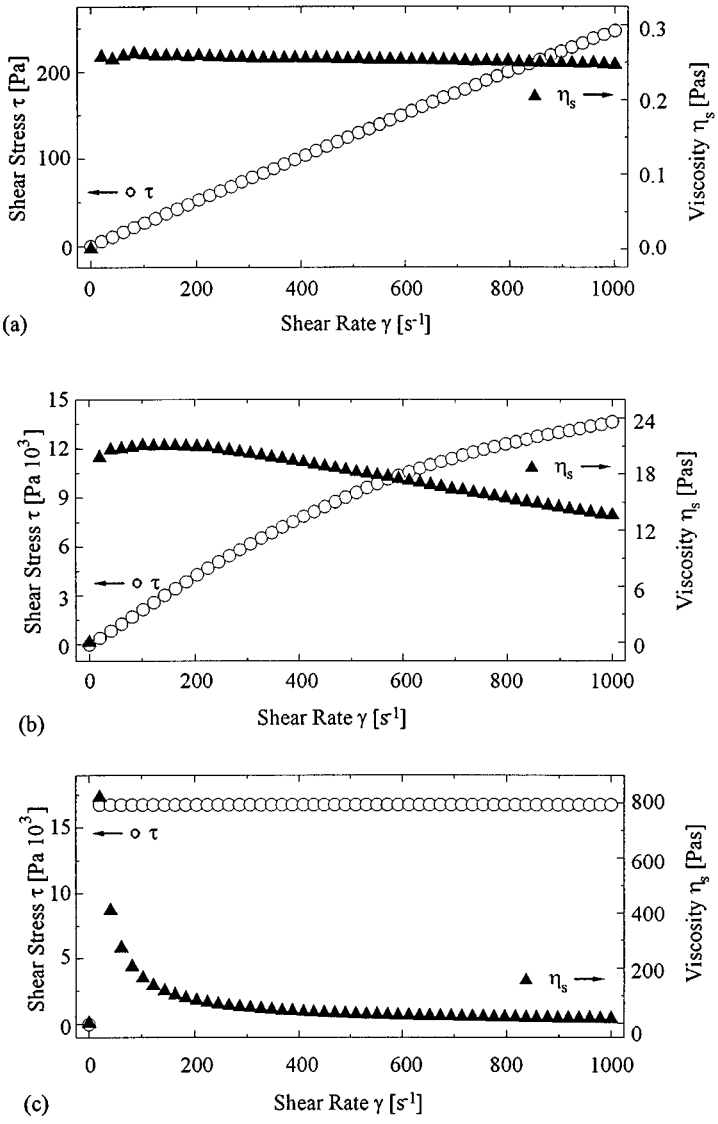

Figure 5 Rheological behaviour of silazanes with different degrees of branching: (a) **S2a**, 1:10; (b) **S2d**, 1:1; (c) **S2e**, 1:05.

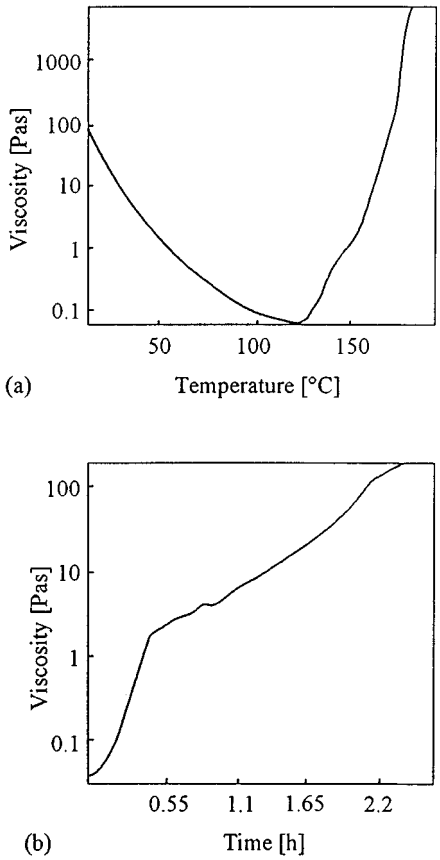

Figure 6 Viscosity of the branched precursor **S2d** as a function of (a) temperature and (b) time; $T = 120$ °C.

from transamination reactions, specific functional groups (Si—H, Si—CH=CH_2) may be used to support thermosetting (Fig. 7a). Crosslinking via hydrosilylation is thermally activated and was responsible for the increase in viscosity. At temperatures above 250 °C this reaction came to an end and unmeltable resins were formed (Fig. 7b).

Thermal analysis

If organometallic precursors are pyrolysed, fragmentation of the oligomer/polymer structure occurs and gaseous species (NH_3, CH_4, H_2) are evolved. This leads to a weight loss, reducing the ceramic yield (=weight of residue after pyrolysis × 100%/weight of liquid silazane). For a suitable pre-ceramic compound this loss should be small (<30 wt%).

In Table 4, the weight loss of the silazanes heated to 1000 °C in an argon atmosphere is shown. For the unbranched precursors the ceramic yield was very low (<11 wt%), and precursors **S1a** and **S1c** evaporated completely. At lower heating rates, the yield increased slightly to 30 wt% for precursor **S1d**, but was still not satisfactory. The loss is due to the low molecular weight of the species and an insufficient degree of crosslinking; thus, most of the silazanes evaporated before ceramization (Fig. 8a).

For branched silazanes the pyrolysis behaviour changed dramatically (Table 4; Fig. 8b). Ceramic yields of 51–77 wt% were achieved. A first weight loss was observed at 150–300 °C. Even for low degrees of branching (D.B.≈10%, precursor **S2a**) the weight loss was reduced from >80 wt% (unbranched precursors) to 28 wt% at this stage. Increasing the degree of branching (D.B.=30–70%) led to a minimal loss of about 10 wt% ($T \leqslant 300$ °C). The branching of the molecules leads to a higher molecular weight and to a higher boiling temperature of the precursor; thus thermosetting is completed before small molecules can evaporate.

A second temperature range of weight loss was observed at 300 °C<T<700 °C for precursors with a low degree of branching (**S2a**, **S2b**). It shifted to higher temperatures, 500 °C<T<800 °C (precursors **S2c**–**S2e**), for higher degrees of branching, yielding ceramic residues of up to 77 wt% (**S2d**). Because of the instability of hydrogen bonds (C–H, N–H, Si–H), the organometallic polymer transforms into an inorganic solid and this transformation is accompanied by a structural rearrangement of the Si–C–N network. Weight loss (about 15 wt%) at these stages is attributed to the evolution of NH_3, CH_4 and H_2, leaving an amorphous Si–C–N material with a low hydrogen content.

Structural changes during pyrolysis were monitored by FTIR spectroscopy (Fig. 9). Due to the loss of low-mass molecules such as CH_4, the intensity of the bands corresponding to vibrations of Si—H, N—H, and C—H bonds decreased. After curing at 300 °C, a certain proportion of Si—H and CH=CH_2 functionalities remained in the resin (Fig. 9a), indicating that hydrosilylation was incomplete. The organic/inorganic transition was observed in the temperature range from 300 to 600 °C (Fig. 9b–e). At 800 °C this process was completed and

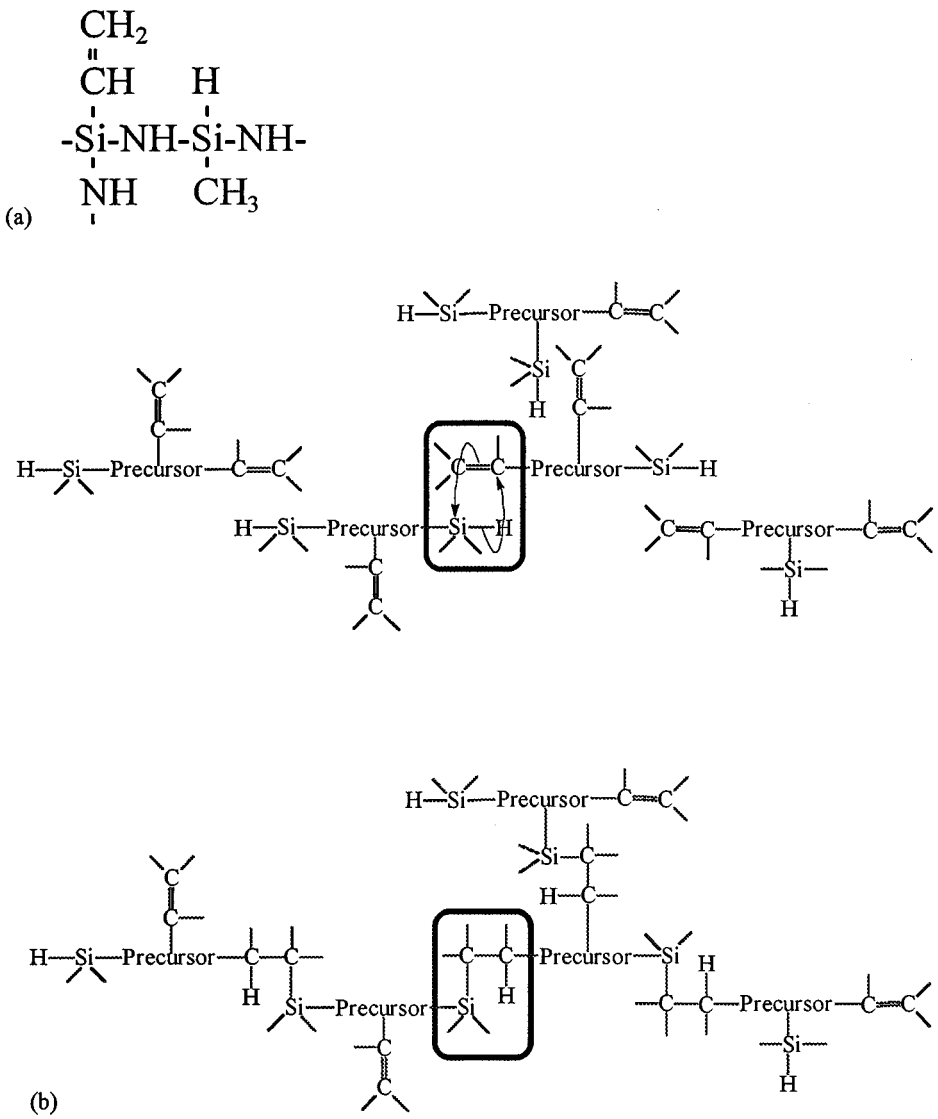

Figure 7 (a) Monomeric unit. (b) Crosslinking of oligomeric silazanes by hydrosilylation reactions.

Table 4 Ceramic yield of the unbranched (**S1a**–**S1d**) and the branched precursors (**S2a**–**S2e**) (1000 °C, 5 K min^{-1}, Ar)

S1a	**S1b**	**S1c**	**S1d**	**S2a**	**S2b**	**S2c**	**S2d**	**S2e**
Ceramic yield[a] (%)	—	11	—	10–30[b]	51	61	71	77	75

[a] Ceramic yield = $100 \times m/m_0$ where m = mass of residue after pyrolysis, m_0 = mass of liquid silazane.
[b] Different heating rates (see text).

further structural changes were not detectable by FTIR spectroscopy.

Further weight loss was noticed on heating the pyrolysed materials to 1800 °C. It was attributed to the decomposition reactions represented in Eqns [2] and [3]. Theoretical temperatures at equilibrium were calculated from thermodynamic data.[18]

$$Si_3N_4 + 3C \rightarrow 3SiC + 2N_2 \quad T_1 = 1438\ °C \quad [2]$$

$$Si_3N_4 \rightarrow 3Si + 2N_2 \quad T_2 = 1823\ °C \quad [3]$$

In contrast to conventionally produced silicon nitride powder, which decomposes continuously, polymer-derived Si–C–N ceramics exhibited a sharp decomposition temperature. Depending on the content of free carbon, Si_3N_4 decomposed forming SiC according to Eqn [2]. At 1500 °C, two-thirds of the maximum weight loss (36 wt% at 1800 °C) was observed and nitrogen was completely eliminated (in an argon atmosphere). This result is in agreement with the chemical analysis of the amorphous Si–C–N ceramic (Si, 48.7; N, 27.4; C, 20.8; H, 0.84; O, 0.81 wt%$\rightarrow Si_1C_{0.99}N_{1.13}H_{0.48}O_{0.03}$) from which a

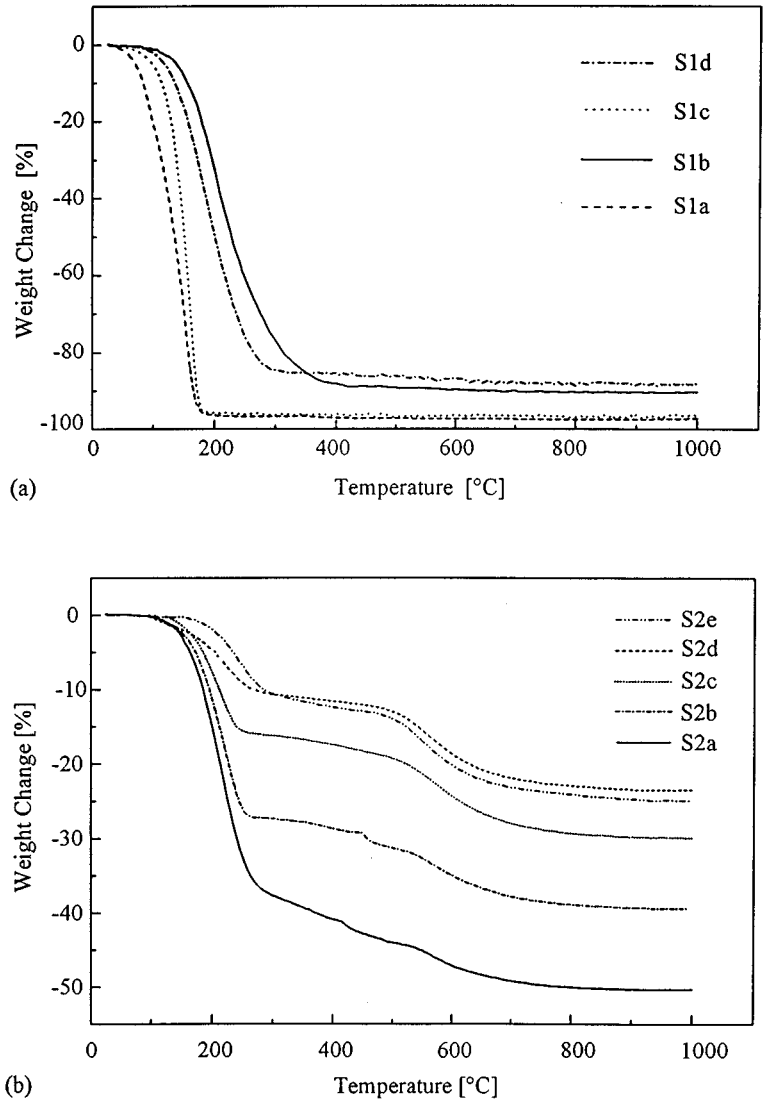

Figure 8 Thermogravimetric analysis of (a) the unbranched precursors **S1a**–**S1d** and (b) the branched precursors **S2a**–**S2d** (5 K min^{-1}, Ar).

possible maximum weight loss of 30 wt% was calculated. In a nitrogen atmosphere, the temperature of decomposition was about 100 K higher. If pyrolysis was performed in ammonia, the weight loss was lower than in argon but carbon was not removed completely due to the formation of stable Si—C—Si bonds by curing the silazanes via hydrosilylation. Furthermore, elemental silicon evaporated and may react with excess carbon to yield SiC. To prevent weight loss, which may lead to either crystallization (see below), porosity or cracking, the maximum application temperature for the amorphous materials should be less than 1500 °C.

Crystallization

Crystalline phases were observed above 1300 °C. Below this temperature the pyrolysed materials appeared to be amorphous to X-rays, in agreement to the results of other groups.[12b] Depending on the structure and chemical composition as well as on the pyrolysis parameters, different amounts of silicon carbide and nitride were formed. Due to its high ceramic yield and controllable viscosity the precursor **S2d** was chosen to study the crystallization behaviour as a function of temperature and pyrolysis parameters.

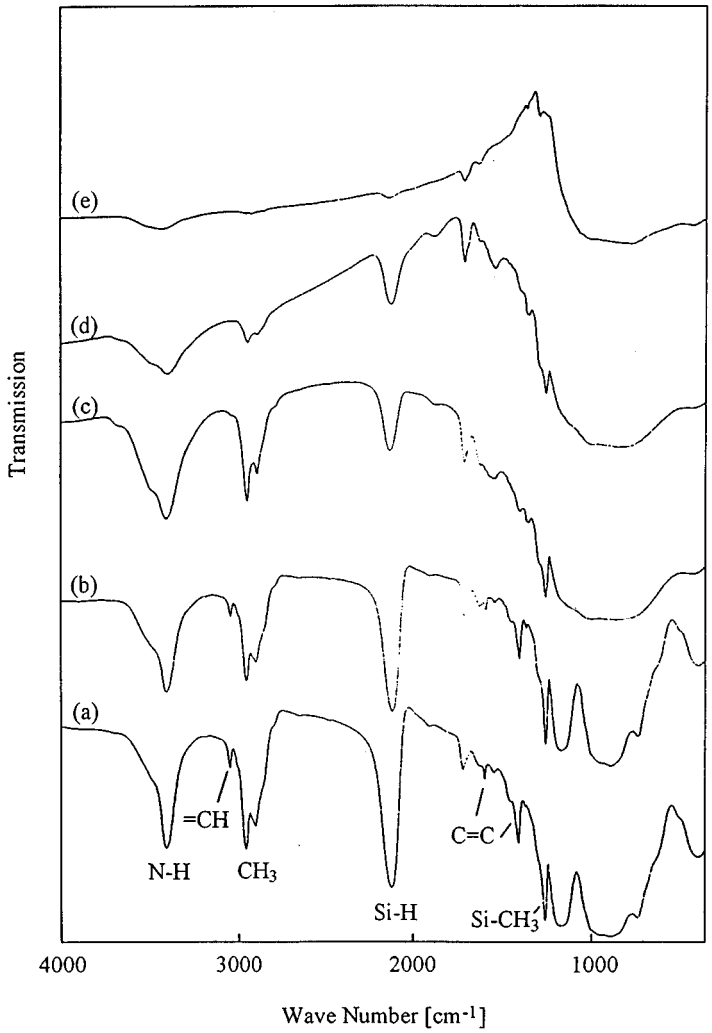

Figure 9 FTIR spectra of pyrolysed samples of the silazane **S2d** at different temperatures: (a) 300 °C; (b) 500 °C; (c) 550 °C; (d) 600 °C; (e) 800 °C.

The crystallization behaviour in argon from 1400 to 1800 °C is shown in Fig. 10. The pyrolysed materials remained amorphous up to 1400 °C. The first peaks in the diffraction pattern were observed at 1500 °C. Peak width and intensity indicated a small crystallite size which was nearly the same at 1600 °C. Coarsening of the crystallites was observed at higher temperatures, resulting in a fully crystalline material at 1800 °C.

Evaluation of the powder diffraction pattern showed the formation of β-SiC. Neither α-SiC polytypes nor Si_3N_4 were observed. Carbon may be present, but was still amorphous and could not be detected. In accordance with the thermogravimetric results, no nitrogen-containing phases could be identified. The amorphous ceramic decomposed before Si_3N_4 crystallized.

If nitrogen or ammonia was used during pyrolysis, the formation of crystalline silicon nitride was observed (Fig. 11). In a small temperature range (1500–1550 °C, Fig. 11b–d), silicon nitride crystallized as was expected from the nitrogen content of the Si–C–N ceramic (Eqn [4]). The molar ratio Si_3N_4/SiC was calculated from the chemical analysis of the amorphous pyrolysis residue to be approximately 2:1, with the assumption that the nitrogen content was completely transformed to Si_3N_4 and the remaining silicon was transformed to SiC.

$$Si_{3.54}N_{4.00}C_{3.51} \rightarrow Si_3N_4 + 0.54\ SiC + 2.97\ C_{free} \quad [4]$$

At higher temperatures ($\geqslant$1600 °C) formation of silicon carbide was predominant (Fig. 11e) due to either carbothermic reduction of Si_3N_4 (Eqn [2]) or decomposition of Si_3N_4 (Eqn [3]), and subsequent reaction of silicon with excess carbon (in the case of samples pyrolysed in a nitrogen atmosphere).

Ceramic matrix composites via infiltration and pyrolysis

For composite processing, precursor **S2d** was used as the matrix constituent due to its high ceramic yield and low viscosity. A SiC-based fibre (Nicalon® 202) was selected as reinforcing element. The fibre filaments were coated with 80 nm of CVD carbon to adjust the interface properties. Fibre rovings (6000 filaments) were fixed in a semi-closed brass mould (8 mm × 4 mm × 100 mm) and the precursor was added drop-wise, yielding a fibre/matrix volume ratio of 1:1. The composite was cured at 250 °C and subsequently pyrolysed at 1000 °C in argon. In order to achieve a dense matrix, multiple infiltration and pyrolysis steps had to be performed.

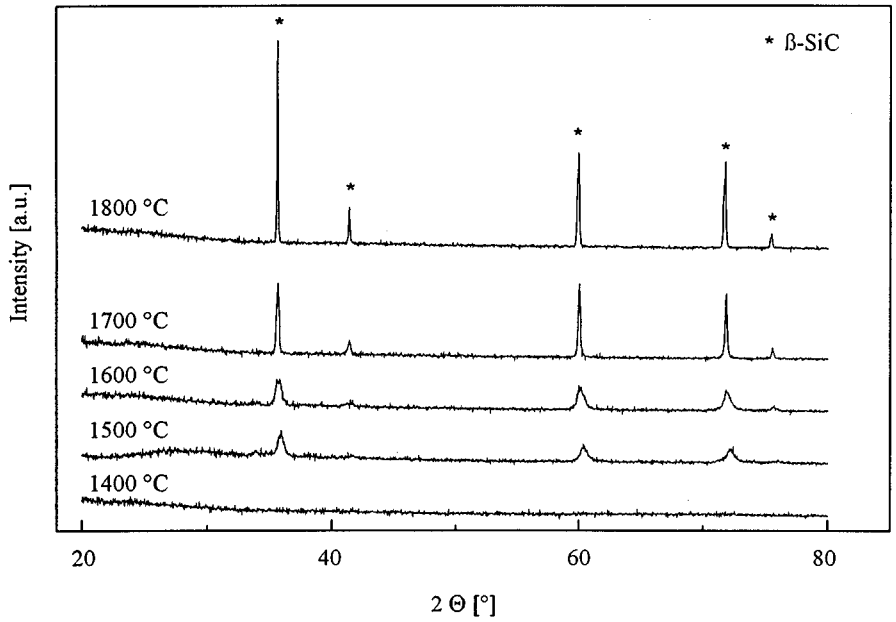

Figure 10 X-ray powder diffraction patterns of the pyrolyzed precursor **S2d** annealed at different temperatures (10 K min^{-1}, Ar, 6 h).

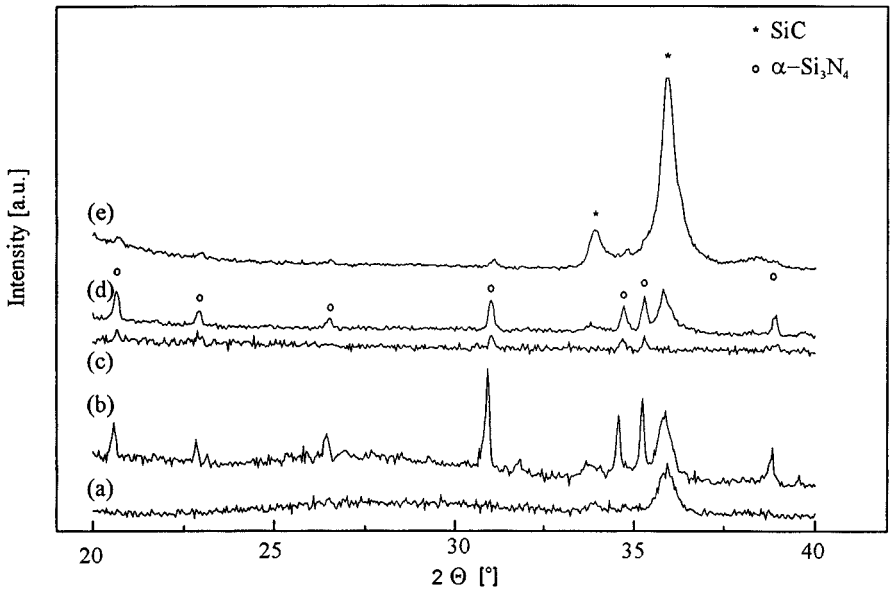

Figure 11 X-ray powder diffraction patterns of pyrolysed precursor **S2d** at different temperatures (10 K min^{-1}, 6 h) and in various atmospheres: (a) 1500 °C, Ar; (b) 1500 °C, NH_3/N_2; (c) 1500 °C, N_2; (d) 1550 °C, N_2; (e) 1600 °C, N_2.

Figure 12 shows an SEM picture of a composite section (open porosity 5.9%) that has been infiltrated and pyrolysed five times, the homogeneous grey areas being the SiC fibres and the dark and bright shaded grey areas being the SiCN matrix. The sections that appear lighter can be attributed to the ceramic residue after the first impregnation cycle. Some residual porosity, which cannot be eliminated even by further infiltration and pyrolysis steps (open porosity after ten steps: 2.0%), is still present. Figure 13 demonstrates qualitatively the damage-tolerant behaviour of a composite material, showing pull-out of single fibres from the matrix with pull-out lengths > 200 μm. The complete results of the composite preparation and characterization will be published in a subsequent paper.

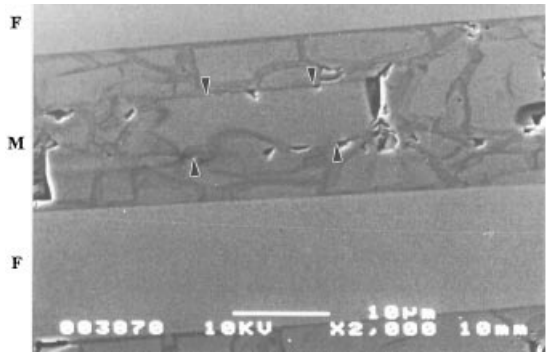

Figure 12 SEM micrograph of a polished composite section showing the different processing steps of matrix built up: F, fibre; M, matrix; the arrowheads indicate the matrix from the first pyrolysis step.

CONCLUSIONS

The careful maintenance of synthesis parameters enables the control of important properties of the silazanes studied (viscosity, ceramic yield, phase

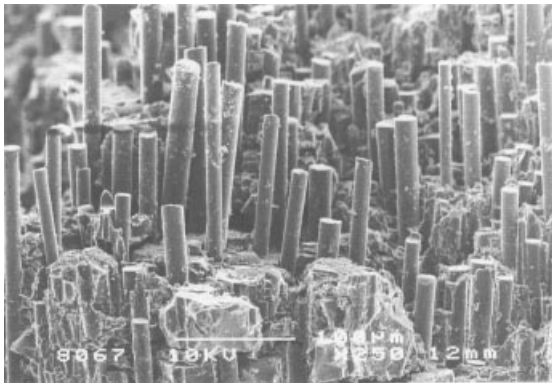

Figure 13 SEM micrograph of the composite fracture surface, with extensive pull-out.

composition). By varying the chemical substituents and the structure of the silazanes, the C/N ratio in the ceramic matrix could be changed over a wide range. With a high proportion of vinyl groups, carbon-rich residues were achieved, whereas branching of the oligomers, as well as an NH_3/N_2 atmosphere during pyrolysis, led to a higher nitrogen content.

Design of the molecular structure led to precursors with both the required stability and reactivity. A low degree of branching was responsible for a high long-term stability whereas functional groups attached to the molecues led to a latent reactivity. Intra- and/or inter-molecular mixtures of Si—CH=CH_2— and Si—H substituents allowed stabilization of the polymer via hydrosilylation after moulding. The viscosity values were low due to low molecular weights; nevertheless, ceramic yields could be increased to 77 wt%, controlled by the degree of branching of the Si–N backbone.

Because of the low viscosity, fibre-reinforced CMCs could be fabricated from the liquid precursors even at room temperature without the use of a solvent or pressure. No fibre damage was observed during the pyrolysis of the composites at temperatures up to 1000 °C.

Future synthesis strategies with respect to ternary Si–C–N precursors will focus on two-component thermosetting systems. Ternary and quarternary systems including non-oxide as well as oxide systems are being investigated, with the emphasis on Si–M–C–N (M=Ti, Zr, Hf) precursors.[19] Furthermore, the potential of these novel precursors for processing monolithic materials, fibres and nano/micro and hybrid composites[16] will be investigated.

Acknowledgements The authors thank the Deutsche Forschungsgemeinschaft and the Bayerisches Wirtschaftsministerium for financial support.

REFERENCES

1. J. K. Wynne and R. W. Rice, *Annu. Rev. Mater. Sci.* **14**, 297 (1984).
2. M. Peuckert, T. Vahs and M. Brück, *Adv. Mater.* **2**, 398 (1990).
3. J. Bill and F. Aldinger, *Adv. Mater.* **7**, 775 (1995).
4. A. Stock and K. Somieski, *Ber. Dtsch. Chem. Ges.* **54**, 740 (1921).
5. U. Wannagat, *Adv. Inorg. Chem.* **6**, 225 (1964).
6. B. J. Aylett, *Organomet. Chem. Rev.* **3**, 151 (1968).
7. W. Verbeek, German Patent DE 2218960 (1973).
8. S. Yajima, K. Okamura, J. Hayashi and M. Omori, *J. Am. Ceram. Soc.* **59**, 324 (1975).
9. D. Seyferth, C. Strohmann, H. J. Tracy and J. L. Robison, *Mater. Res. Soc. Symp.* **249**, 1 (1992).
10. R. M. Laine, Y. D. Blum, D. Tse and R. Glaser, Synthetic routes to oligosilazanes and polysilazanes: polysilazane precursors to silicon nitride. In: *Inorganic and Organometallic Polymers*, Zeldin, M., Wynne, K. J. and Allcock, H. R., American Chemical Society, Am. Chem. Soc. Symp. Ser. 360, Washington DC, 1988, p.124.
11. M. Birot, J.-P. Pillot and J. Dunogues, *Chem. Rev.* **95**, 1443 (1995).
12 (a) D. Bahloul, M. Pereira and P. Goursat, *J. Am. Ceram. Soc.* **76**, 1156 (1993); (b) *idem*, *ibid.* **76**, 1163 (1993).
13. J. Lücke, M. Keuthen and G. Ziegler, *Ceram. Proc. Sci. Technol.* **51**, 205 (1994).
14. R. Riedel, M. Seher, J. Mayer and D. V. Szabo, *J. Eur. Ceram. Soc.* **15**, 703 (1995).
15. P. Greil, *J. Am. Ceram. Soc.* **78**, 835 (1995).
16. G. Ziegler, J. Hapke and J. Lücke, *Ceram. Trans.* **58**, 13 (1995).
17. G. Ziegler, M. Keuthen, J. Lücke and G. H. Wroblewska, Polymer-derived fiber-reinforced ceramic matrix composites and CMCs produced by powder processing: state of the art and future aspects. In: *Proc. 10th Int. Conf. Composite Materials*, Poursartip, A. and Street, K. (eds), Woodhead, Cambridge, Vol. IV, p. 561.
18. I. Barin, *Thermochemical Data of Pure Substances, Parts I and II*, 2nd edn, VCH, Stuttgart, 1993.
19. J. Hapke and G. Ziegler, *Adv. Mater.* **7**, 380 (1995).